

Scattering of a TM Wave from a Periodic Surface with Finite Extent: Undersampling Approximation

Junichi NAKAYAMA^{†a)} and Yasuhiko TAMURA[†], Members

SUMMARY This paper deals with the scattering of a TM plane wave from a perfectly conductive sinusoidal surface with finite extent. For comparison, however, we briefly discuss the diffraction by the sinusoidal surface with infinite extent, where we use the concept of the total diffraction cross section per unit surface introduced previously. To solve a case where the sinusoidal corrugation width is much wider than wave length, we propose an undersampling approximation as a new numerical technique. For a small rough case, the total scattering cross section is calculated against the angle of incidence for several different corrugation widths. Then we find remarkable results, which are roughly summarized as follows. When the angle of incidence is apparently different from critical angles and diffraction beams are all scattered into non-grazing directions, the total scattering cross section increases proportional to the corrugation width and hence the total scattering cross section per unit surface (the ratio of the total scattering cross section to the corrugation width) becomes almost constant, which is nearly equal to the total diffraction cross section per unit surface in case of the sinusoidal surface with infinite extent. When the angle of incidence is critical and one of the diffraction beams is scattered into a grazing direction, the total scattering cross section per unit surface strongly depends on the corrugation width and approximately approaches to the total diffraction cross section per unit surface as the corrugation width gets wide.

key words: numerical analysis, undersampling, Wood's anomaly, total scattering cross section, multiple scattering

1. Introduction

This paper deals with the wave scattering of a TM plane wave from a perfectly conductive sinusoidal surface with finite extent (see Fig. 1). For numerical analysis, we propose a new approximation method which is practically useful when the surface is small in roughness but the corrugation width W is much larger than λ the wave length.

When a TM plane wave is incident on a perfectly conductive periodic surface with finite extent, strong scattering takes place into directions determined by the grating formula and the scattered wave becomes a sum of diffraction beams [1], [2]. When the angle of incidence θ_i is critical, one of the diffraction beams is scattered into a grazing direction. Such a diffraction beam is scattered by the surface corrugation and re-scattered again. Thus, a multiple scattering takes place. This multiple scattering may be weak when the corrugation width W is not wide but becomes strong when W is wide enough. Therefore, it is physically expected that the corrugation width W gives serious effects to the scattering properties. When the corrugation width W goes to infinity

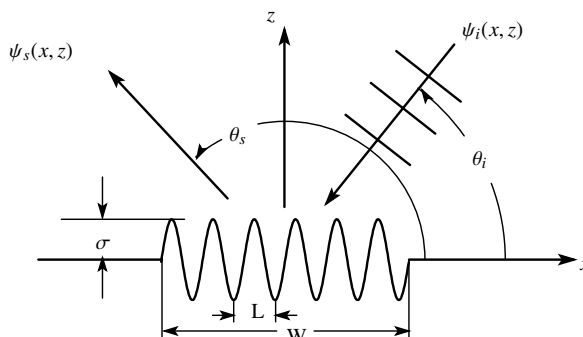


Fig. 1 The scattering of a TM plane wave from a periodic surface with finite extent. $\psi_i(x, z)$ and $\psi_s(x, z)$ are the incident plane wave and the scattered wave, respectively. θ_i and θ_s are the angle of incidence and a scattering angle, respectively. L is the period. W and σ are the width and roughness of the surface, respectively.

and the surface becomes perfectly periodic*, such a multiple scattering causes a well known Wood's anomaly [9]–[11]. However, the effect of multiple scattering has not been discussed in details for a periodic surface with finite extent.

In order to discuss the multiple scattering effect, we have to deal with a case where W is much larger than λ the wave length. But theoretical or numerical methods have not been developed yet for such a case. When the angle of incidence is critical, the small perturbation method gives the total scattering cross section per unit surface proportional to \sqrt{W} asymptotically and causes unphysical divergence at $W \rightarrow \infty$ [12], which is the same drawback as in the Rayleigh-Rice theory of periodic grating [13], [14]. On the other hand, numerical methods [1], [2], [15]–[17] commonly reduce the scattering problem to solving a matrix equation. Roughly speaking, the matrix is $[8W/\lambda] \times [8W/\lambda]$ in size. This fact makes it impractical to solve a case with W

* The words, *the perfectly periodic surface*, are an analogy of *the perfect lattice or perfect crystal* in the solid state physics [3]. In our opinion, periodic surfaces may be classified into two categories. One is the perfectly periodic surface, which is described by a periodic function in strictly sense. The other is the imperfect periodic surface, which is periodic in some sense but has imperfections. Some examples are a periodic surface with finite extent, a periodic surface with apodisation [4], a periodic surface with defects [5], and periodic random surface [6]–[8]. In this paper, we intend to clarify properties of the scattering from a periodic surface with finite extent in comparison with the perfectly periodic case, where the perfectly periodic case is regarded as an idealized standard.

Manuscript received May 11, 2006.

Manuscript revised August 9, 2006.

[†]The authors are with the Graduate School of Engineering and Design, Kyoto Institute of Technology, Kyoto-shi, 606-8585 Japan.

a) E-mail: nakayama@kit.ac.jp

DOI: 10.1093/ietele/e90-c.2.304

much larger than λ the wave length, because of increasing computation time.

To deal with a case $W/\lambda > 10^3$, we need a new method for numerical analysis. We propose an undersampling approximation, by which the matrix size is reduced to about $[4L/\lambda + 1] \times [4L/\lambda + 1]$, L being the surface period. By use of this approximation, we calculate the total scattering cross section for W/λ up to 6.4×10^3 . Then, we find that, when the angle of incidence is apparently different from a critical angle, the total scattering cross section per unit surface is almost constant independent of W . When the angle of incidence is critical, however, the total scattering cross section per unit surface depends on W due to the multiple scattering.

2. Formulation

Let us consider the scattering of TM plane wave from a perfectly conductive sinusoidal surface with finite extent shown in Fig. 1. We write the surface corrugation as

$$z = f(x) = \sigma u(x|W) \sin(k_L x), \quad k_L = \frac{2\pi}{L}, \quad (1)$$

where L is the period, k_L is the spatial angular frequency of the period L , W is the width of corrugation which is implicitly assumed to be an integer multiple of the period L to make $f(x)$ continuous at $x = \pm W/2$. $u(x|W)$ is a rectangular pulse,

$$u(x|W) = u^2(x|W) = \begin{cases} 1, & |x| \leq W/2 \\ 0, & |x| > W/2 \end{cases}, \quad (2)$$

and σ is the surface roughness. In what follows, we only consider a case with $\sigma \ll \lambda$, λ being wave length. We denote the y component of the magnetic field by $\psi(x, z)$, which satisfies the wave equation

$$\left[\frac{\partial^2}{\partial x^2} + \frac{\partial^2}{\partial z^2} + k^2 \right] \psi(x, z) = 0, \quad (3)$$

in the region $z > f(x)$ and the Neumann condition on the surface (1)

$$\left[\frac{\partial}{\partial z} - \frac{df}{dx} \frac{\partial}{\partial x} \right] \psi(x, z) \Big|_{z=f(x)} = 0. \quad (4)$$

Here, $k = 2\pi/\lambda$ is wave number. We write the incident plane wave $\psi_i(x, z)$ as

$$\psi_i(x, z) = e^{-ipx} e^{-i\beta(p)z}, \quad p = k \cdot \cos \theta_i, \quad (5)$$

where θ_i is the angle of incidence (see Fig. 1) and $\beta(p)$ is a function of p defined by

$$\begin{aligned} \beta(p) &= \sqrt{k^2 - p^2}, \\ \text{Re} [\beta(p)] &\geq 0, \quad \text{Im} [\beta(p)] \geq 0. \end{aligned} \quad (6)$$

Here, Re and Im are real and imaginary part, respectively. Since the surface is flat for $|x| > W/2$, we put

$$\psi(x, z) = \psi_i(x, z) + e^{-ipx} e^{i\beta(p)z} + \psi_s(x, z), \quad (7)$$

where the second term in the right-hand side is the specularly reflected wave and $\psi_s(x, z)$ is the scattered wave due to the surface roughness. In far region, $\psi_s(x, z)$ becomes a cylindrical wave satisfying the Sommerfeld radiation condition, and hence its Fourier spectrum has singularities but its angular spectrum is always finite [16]. Taking this fact and assuming the Rayleigh hypothesis, we write an approximate expression of $\psi_s(x, z)$ as

$$\psi_s(x, z) = \int_{-k_B}^{k_B} \frac{A_\beta(s)}{\beta(p+s)} e^{-i(p+s)x + i\beta(p+s)z} ds, \quad (8)$$

which is made up of up-going waves and evanescent waves. Here, k_B is a truncated band width, $A_\beta(s)$ is the angular spectrum and is the amplitude of the partial wave scattered into $\theta_s = \Theta(p+s)$ direction, where $\Theta(p+s)$ is defined by

$$\Theta(p+s) = \arccos[-(p+s)/k]. \quad (9)$$

If we put $s = mk_L$, ($m = 0, \pm 1, \pm 2, \dots$), this becomes a famous grating formula [9] for a perfectly periodic surface,

$$\Theta(p + mk_L) = \arccos[-(p + mk_L)/k], \quad (10)$$

where $\Theta(p + mk_L)$ is the m th order diffraction angle.

The optical theorem is analogous to the famous forward scattering theorem and may be written as [2], [16],

$$p_c = p_{inc}, \quad (11)$$

$$p_c = -\frac{4\pi}{k} \text{Re}[A_\beta(0)], \quad (12)$$

$$p_{inc} = \frac{2\pi}{k} \int_{-k_B}^{k_B} \text{Re}[\beta(p+s)] \left| \frac{A_\beta(s)}{\beta(p+s)} \right|^2 ds \quad (13)$$

$$= \frac{W}{2\pi} \int_0^\pi \sigma_s(\theta_s|\theta_i) d\theta_s, \quad (14)$$

$$\sigma_s(\theta_s|\theta_i) = \frac{4\pi^2}{kW} |A_\beta(-k \cos \theta_s - k \cos \theta_i)|^2. \quad (15)$$

Here, $\sigma_s(\theta_s|\theta_i)$ is the differential scattering cross section per unit surface. The optical theorem (11) states that the total scattering cross section p_{inc} is equal to p_c the loss of the amplitude of the partial wave scattered into the specularly reflection direction. Because of (11), however, we will call p_c the total scattering cross section. Further, we will consider p_c/W the total scattering cross section per unit surface in what follows. We note that p_c/W and $\sigma_s(\theta_s|\theta_i)$ are dimensionless.

The optical theorem may be used to estimate the accuracy of an approximate solution. We define the error E_{rr} with respect to the optical theorem as,

$$E_{rr} = \left| \frac{p_c - p_{inc}}{p_c} \right|, \quad (16)$$

which will be calculated below.

3. Rayleigh Hypothesis and Undersampling Approximation

Let us obtain a representation of the angular spectrum by use

of an undersampling approximation. Since $\partial\psi_s/\partial z|_{z=0} = 0$ for $|x| > W/2$ by (1), (5) and (7), we obtain from (4),

$$\begin{aligned} \left. \frac{\partial\psi_s}{\partial z} \right|_{z=0} &= i \int_{-k_B}^{k_B} A_\beta(s') e^{-i(p+s')x} ds' \\ &= \begin{cases} ie^{-ipx} Q(x) & |x| \leq W/2 \\ 0, & |x| > W/2 \end{cases}, \end{aligned} \quad (17)$$

where $Q(x)$ is an unknown function. If $Q(x)$ is square integrable, it can be represented by a Fourier series with period W [1]. However, we approximately expand it as a periodic function with the period L and we put,

$$Q(x) = \sum_{n=-N_Q}^{N_Q} Q_n \cdot e^{-ink_L x}, \quad (18)$$

where L and k_L are the period and the spatial angular frequency introduced in (1), respectively. N_Q is a sufficiently large truncation number and $\{Q_n\}$ is a vector to be determined.

Multiplying $e^{i(p+s)x}$ to (17), integrating the result and using (18), we obtain

$$A_\beta(s) = \frac{1}{2\pi} \sum_{n=-N_Q}^{N_Q} Q_n U(s - nk_L|W), \quad (19)$$

which holds for $|s| \leq k_B$. Here, $U(s|W)$ is the Fourier transform of $u(x|W)$.

$$U(s|W) = \int_{-\infty}^{\infty} u(x|W) e^{isx} dx = \frac{\sin(sW/2)}{(s/2)}, \quad (20)$$

$$\lim_{W \rightarrow \infty} U(s|W) = 2\pi\delta(s), \quad (21)$$

where $\delta(s)$ is the Dirac delta. Since W is an integer multiple of the period L , we obtain $U(nk_L|W) = W\delta_{n0}$, δ_{mn} being Kronecker's delta. Then, we obtain from (19)

$$A_\beta(nk_L) = \frac{W}{2\pi} Q_n, \quad (n = 0, \pm 1, \pm 2, \dots, \pm N_Q) \quad (22)$$

Eq. (19) is an undersampling approximation of the angular spectrum $A_\beta(s)$. Substituting (19) into (8) yields

$$\begin{aligned} \psi_s(x, z) &= \sum_{n=-N_Q}^{N_Q} \frac{Q_n}{2\pi} \int_{-k_B}^{k_B} \frac{U(s - nk_L|W)}{\beta(p + s)} \\ &\quad \times e^{-i(p+s)x + i\beta(p+s)z} ds. \end{aligned} \quad (23)$$

3.1 Equation for $\{Q_n\}$

Let us derive an equation for the vector $\{Q_n\}$. We first introduce a Fourier coefficient $C_m(\alpha, \beta)$ by the relation

$$\begin{aligned} \left[\frac{\partial}{\partial z} - \frac{df}{dx} \frac{\partial}{\partial x} \right] e^{-i\alpha x + i\beta z} \Big|_{z=\sigma \sin(k_L x)} \\ = i \sum_{m=-\infty}^{\infty} C_m(\alpha, \beta) e^{-i\alpha x - imk_L x}. \end{aligned} \quad (24)$$

Using the formula on Bessel function $J_m(z)$,

$$e^{iz \sin(x)} = \sum_{m=-\infty}^{\infty} J_m(z) e^{imx}, \quad (25)$$

we obtain

$$\begin{aligned} C_m(\alpha, \beta) &= \beta J_{-m}(\sigma\beta) \\ &\quad + \frac{\sigma\alpha k_L}{2} [J_{1-m}(\sigma\beta) + J_{-1-m}(\sigma\beta)]. \end{aligned} \quad (26)$$

Substituting (23) into (4) and using (24), we obtain

$$\begin{aligned} \frac{i}{2\pi} \sum_{n=-N_Q}^{N_Q} Q_n \sum_{m=-\infty}^{\infty} \int_{-k_B}^{k_B} \frac{U(s - nk_L|W)}{\beta(p + s)} \\ \times C_m(p + s, \beta(p + s)) e^{-isx - imk_L x} ds \\ = -i \sum_m [C_m(p, -\beta(p)) + C_m(p, \beta(p))] e^{-imk_L x}, \end{aligned} \quad (27)$$

which holds for $|x| < W/2$. Multiplying $e^{ik_L x}$ to the both sides of this equation, and integrating over an interval $[-W/2, W/2]$, one easily gets a set of equations for the vector $\{Q_l\}$,

$$\sum_{n=-N_Q}^{N_Q} D_{ln}(p) Q_n = E_l(p), \quad (28)$$

$$\begin{aligned} D_{ln}(p) &= \sum_{m=-\infty}^{\infty} \int_{-k_B}^{k_B} \frac{U(s - nk_L|W)}{2\pi W\beta(p + s)} C_m(p + s, \\ &\quad \beta(p + s)) U(s + (m - l)k_L|W) ds, \end{aligned} \quad (29)$$

$$E_l(p) = -[C_l(p, -\beta(p)) + C_l(p, \beta(p))]. \quad (30)$$

The integrand in (29) has singularities at $p + s = \pm k$. The integral may be evaluated easily by putting $p + s = -k \cos \alpha$ and changing the variable of integration from s to α . When $W/\lambda > 10^3$, however, numerical integration takes much computation time and its highly accurate evaluation becomes difficult technically.

4. Perfect Periodic Case

In the limit $W \rightarrow \infty$, our surface (1) becomes perfectly periodic and hence the scattered wave $\psi_s(x, z)$ is physically expected to converge to the diffracted wave by the perfectly periodic surface. Therefore, we consider the diffraction by the perfectly periodic surface.

As is well known, the wave field has the Floquet form in a perfectly periodic case. According to reference [18], we write

$$\begin{aligned} \psi(x, z) &= e^{-ipx} e^{-i\beta(p)z} + e^{-ipx} e^{i\beta(p)z} \\ &\quad + \sum_{m=-\infty}^{\infty} A_m e^{-i(p+m k_L)x} e^{i\beta(p+m k_L)z}, \end{aligned} \quad (31)$$

where the second term in the right hand side is the reflected wave by a flat surface, and $(A_m + \delta_{m0})$ is the amplitude of the m th order Floquet mode. Note that $(A_0 + 1)$ is the reflection

coefficient.

In the periodic case, we may have two different energy balance formulas [18]. One is the energy conservation relation and the other the optical theorem. Many works have been carried out on the former one, but we are interested in the later one, because we expect that the optical theorem could be a bridge between the scattering from a periodic surface with finite extent and the diffraction by a perfectly periodic surface [1], [2].

We may write the optical theorem as

$$p_c^{(g)} = p_{inc}^{(g)}, \quad (32)$$

$$p_c^{(g)} = -2 \frac{\beta(p)}{k} \text{Re}[A_0], \quad (33)$$

$$p_{inc}^{(g)} = \sum_{m=-\infty}^{\infty} \frac{\text{Re}[\beta(p + mk_L)]}{k} |A_m|^2. \quad (34)$$

Since k in the denominator in (33) and (34) is the incident energy flux, $p_{inc}^{(g)}$ is the total diffraction cross section per unit surface, whereas $p_c^{(g)}$ means the loss of specularly reflection amplitude. Because of (32), however, we will call $p_c^{(g)}$ the total diffraction cross section per unit surface. Note that $p_c^{(g)}$ is dimensionless. In what follows, we will compare $p_c^{(g)}$ with p_c/W the total scattering cross section per unit surface.

It is known in case of a perfectly periodic Neumann surface [19]–[21] that $(1 + A_0)$ becomes -1 and any other diffraction amplitude A_m , ($m \neq 0$), vanishes at a low grazing limit of incidence. Because of the factor $\beta(p) = k \sin \theta_i$, however, $p_c^{(g)}$ vanishes in the limit $\theta_i \rightarrow 0$ as is illustrated later.

5. Optical Theorem as Bridge

We have been looking for bridges between the scattering from a finite periodic surface and the diffraction by a perfectly periodic surface. In previous papers [1], [2], we simply assumed that the total scattering cross section p_c is linearly proportional to W , because the scattering is generated by the surface corrugation with the width W . Such assumption is useful in some cases but is not always valid as is shown later.

As is described above, the scattered wave $\psi_s(x, z)$ is physically expected to converge to the diffracted wave by the perfectly periodic surface in the limit $W \rightarrow \infty$. Mathematically, however, such convergence is doubtful. However, we propose an expectation such that p_c/W the total scattering cross section per unit surface converges to $p_c^{(g)}$ the total diffraction cross section per unit surface. We write our expectation as

$$\lim_{W \rightarrow \infty} \frac{p_c}{W} = p_c^{(g)}, \quad (35)$$

which could be a bridge between the scattering from a finite periodic surface and the diffraction by a perfectly periodic surface. In what follows, we numerically examine this expectation.

6. Numerical Examples

For numerical calculation, we put

$$L = 2.5\lambda, \quad (36)$$

by which $\theta_i = 0^\circ$, 53.130° , and 78.463° become the critical angles of incidence.

6.1 Perfectly Periodic Case

By a non-Rayleigh method [22], we calculated numerically the amplitude A_m in (31) from $m = -8$ to $m = 8$. Then, $p_c^{(g)}$ the total diffraction cross section per unit surface is illustrated against the angle of incidence in Fig. 2. We see that Wood's anomaly appears as rapid changes of $p_c^{(g)}$ at $\theta_i = 53.130^\circ$ and 78.463° . This figure shows that $p_c^{(g)}$ vanishes at low grazing limit $\theta_i \rightarrow 0$ as is described above.

The total diffraction cross section per unit surface $p_c^{(g)}$ strongly depends on the roughness σ except for the critical angles of incidence. It is interesting to see that such dependence becomes very weak at $\theta_i = 53.130^\circ$. Some numerical examples are $p_c^{(g)} = 1.9222$ at $\sigma = 0.01\lambda$, 1.9739 at $\sigma = 0.05\lambda$, 2.1187 at $\sigma = 0.1\lambda$, and 2.4912 at $\sigma = 0.2\lambda$. However, we note that such weak dependence appears only for a sinusoidal surface.

6.2 Finite Periodic Case

To reduce computation time, the truncation number N_Q and the truncated band width k_B should be set as small as possible. Empirically, we set

$$N_Q = \left[\frac{2k}{k_L} \right]_r = \left[\frac{2L}{\lambda} \right]_r, \quad k_B = (N_Q + 1)k_L, \quad (37)$$

where $[]_r$ means round out operation. In case of (36), we have $N_Q = [2 \times 2.5]_r = 5$, so that (28) becomes a

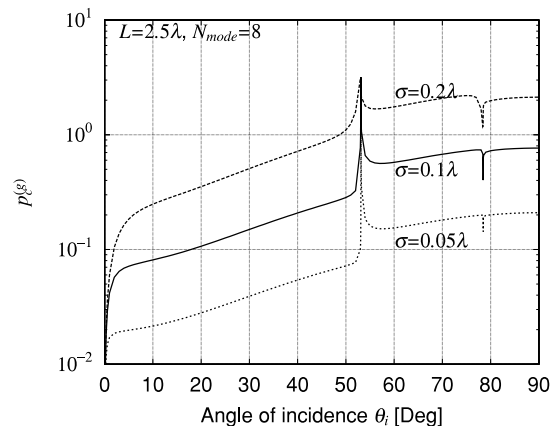


Fig. 2 Total diffraction cross section per unit surface $p_c^{(g)}$ against θ_i the angle of incidence. Perfectly periodic case. $L = 2.5\lambda$. $\sigma = 0.05\lambda$, 0.1λ and 0.2λ .

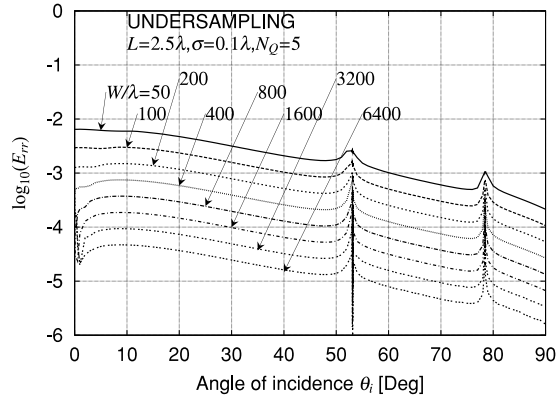


Fig. 3 Error with respect to the optical theorem. $L = 2.5\lambda$, $\sigma = 0.1\lambda$. The error decreases when W becomes large.

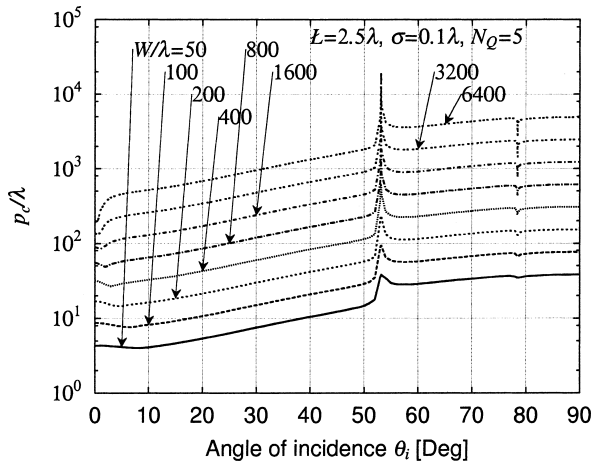


Fig. 4 Total scattering cross section p_c/λ against the angle of incidence θ_i . $L = 2.5\lambda$, $\sigma = 0.1\lambda$.

$(2N_Q + 1) \times (2N_Q + 1) = 11 \times 11$ matrix equation. The matrix equation is solved for $\sigma = 0.1\lambda$, for θ_i from 0.00001° to 90° and for eight different values of W/λ , which are 50, 100, 200, 400, 800, 1600, 3200 and 6400. Here, $W/\lambda = 6400 = 2560 \times 2.5$ means W is 2560 times of the period $L = 2.5\lambda$, for example. By (16), we then calculated E_{rr} in Fig. 3, which shows that the error decreases monotonously with increasing W except for $\theta_i \approx 0$. Even for $W/\lambda = 50$ the error is less than 1% for any angle of incidence. This result suggests that our undersampling approximation and our parameter setting (37) give a reasonable result for a small rough case.

Figure 4 shows the total scattering cross section[†] p_c against θ_i . When θ_i is apparently different from critical angles of incidence, p_c increases linearly proportional to W . At a critical angle $\theta_i \approx 53.130^\circ$, we see peaks which become sharp and clear as W gets large. At another critical angle $\theta_i \approx 78.463^\circ$, we see dips, which become deep and clear when W becomes large. Except for $\theta_i \approx 0$, the curve of p_c for $W/\lambda = 6400$ is quite similar in shape to $p_c^{(g)}$ of the perfectly periodic case. It is interesting to see that curves of p_c against θ_i depend on W and change their shapes when

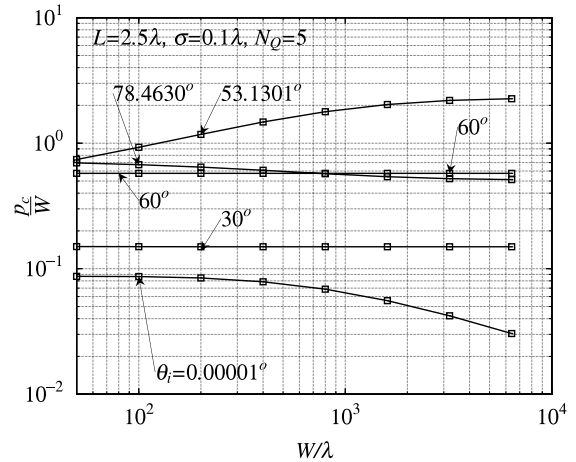


Fig. 5 Total scattering cross section per unit surface p_c/W against the corrugation width W/λ . $L = 2.5\lambda$, $\sigma = 0.1\lambda$.

$\theta_i < 10^\circ$. We note that the behavior of p_c near $\theta_i \approx 0$ is entirely different from $p_c^{(g)}$ in Fig. 2. At a low grazing limit $\theta_i \rightarrow 0$, p_c does not vanish but $p_c^{(g)}$ approaches to zero. This figure suggests that the scattering takes place at a low grazing limit of incidence, whereas the diffraction disappears as is discussed above.

Figure 5 is a main result of this paper. It illustrates p_c/W against W for several different angles of incidence. When θ_i is apparently different from critical angles, for example, when $\theta_i = 30^\circ$, p_c/W is almost constant. Numerical examples for $\theta_i = 30^\circ$ are $p_c/W = 0.1495281$ at $W/\lambda = 1600$, 0.1495190 at 3200 and 0.1495145 at 6400 , whereas $p_c^{(g)} = 0.1495099$ in the perfectly periodic case. When $\theta_i = 60^\circ$, we have $p_c = 0.5751289$ at $W/\lambda = 1600$, 0.5751200 at 3200 and 0.5751153 at 6400 , which are almost equal to $p_c^{(g)} = 0.5751105$. These facts suggest again that our undersampling approximation gives a reasonable solution. Thus, we may conclude that our expectation (35) holds for a non-critical angle of incidence.

If the angle of incidence is critical, p_c/W depends on W . This should be understood as multiple scattering effects. Figure 5 shows that, when $\theta_i = 0.00001^\circ$, p_c/W decreases monotonously as W increases. If the relation (35) holds, however, p_c/W must converge to $p_c^{(g)}$, which is 6.9895×10^{-7} at $\theta_i = 0.00001^\circ$.

When $\theta_i = 53.130^\circ$, p_c/W slowly increases with W and almost saturates for a large value of W . Numerically, $p_c/W = 2.031361$ at $W/\lambda = 1600$, 2.190114 at 3200 , and 2.261195 at 6400 , which is approximately equal to $p_c^{(g)} = 2.1187$ when $\sigma = 0.1\lambda$. For $\theta_i = 78.463^\circ$, p_c/W slowly decreases as W increases. We have $p_c = 0.5407401$ at $W/\lambda = 1600$, 0.5212594 at 3200 and 0.5124105 at 6400 , whereas $p_c^{(g)} = 0.5290224$. These numerical examples show that, for a critical angle of incidence, our expectation (35)

[†]The value p_c by the undersampling approximation is slightly different from that by the spectral formalism [16]. But discrepancies are small. They are, for example, less than 0.7% when $W = 100\lambda$.

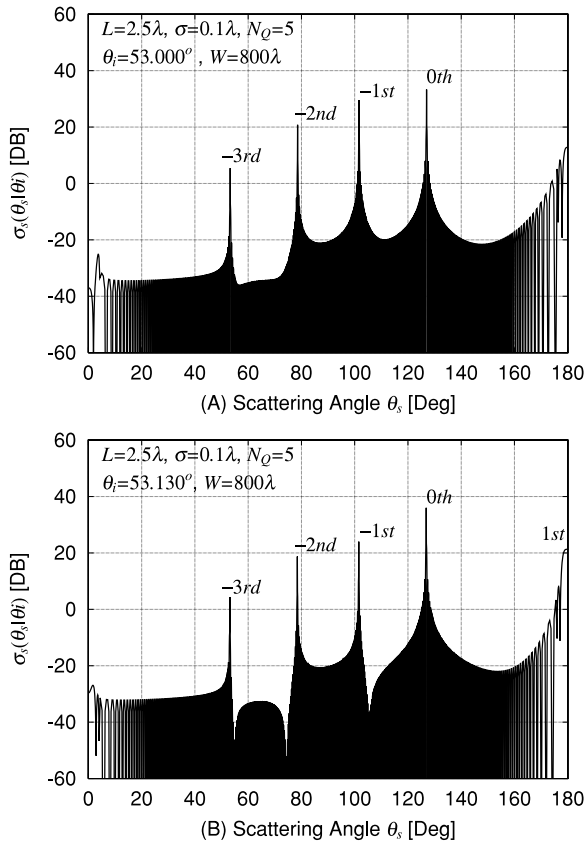


Fig. 6 Scattering cross section against scattering angle θ_s . $L = 2.5\lambda$, $\sigma = 0.1\lambda$. $W = 800\lambda$, (A) $\theta_i = 53.000^\circ$, (B) $\theta_i = 53.130^\circ$.

hold approximately. We suspect that p_c/W converges to p_c with dumping oscillations and small differences between p_c/W and $p_c^{(g)}$ could be caused by such oscillations. But this point is not clear at present and is left for future study.

We have seen in Fig. 4 that a small variation of the incident angle causes a large variation of p_c when θ_i is nearly critical. Let us see some relation of such variations with the differential scattering cross section $\sigma_s(\theta_s|\theta_i)$. Figure 6(A) illustrates $\sigma_s(\theta_s|\theta_i)$ for $W = 800\lambda$, $\sigma = 0.1\lambda$, and a non-critical angle $\theta_i = 53.000^\circ$, where the 0th, -1st, -2nd, and -3rd order diffraction beams appear as peaks at $\theta_s = 127.000^\circ$, 101.643° , 78.569° and 53.260° , respectively. Among these peaks, the 0th order one is the largest with level 33.32 dB. Slightly changing θ_i to a critical angle $\theta_i = 53.130^\circ$, we have $\sigma_s(\theta_s|\theta_i)$ in Fig. 6(B), where the 1st order diffraction beam appears at $\theta_s = 180^\circ$. Comparing Fig. (A) and (B), we see that the 0th order diffraction peak is enhanced to 36.02 dB in the critical case, which is 2.7 dB higher than the 0th order peak in Fig. (A). Since p_c is mainly determined by the largest peak level in $\sigma_s(\theta_s|\theta_i)$, we may conclude that such enhancement of the 0th order diffraction beam makes the peak of p_c at $\theta_i = 53.130^\circ$.

To look for the reason why p_c has a dip at $\theta_i = 78.463^\circ$, we illustrate $\sigma_s(\theta_s|\theta_i)$ for a non-critical angle $\theta_i = 78.000^\circ$ and for a critical angle $\theta_i = 78.463^\circ$ in Fig. 7. In Fig. (A), the -1st order diffraction appears as the largest peak at $\theta_s =$

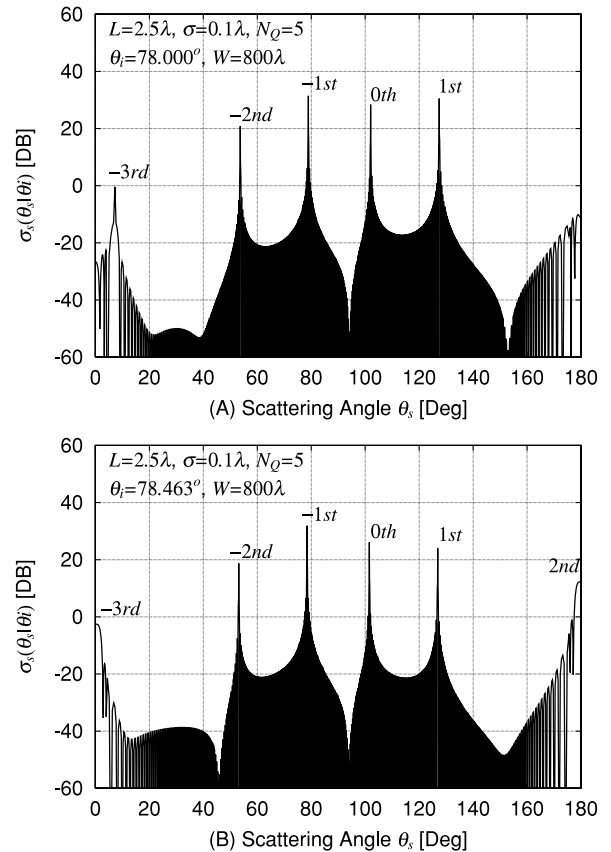


Fig. 7 Scattering cross section against scattering angle θ_s . $L = 2.5\lambda$, $\sigma = 0.1\lambda$. $W = 800\lambda$, (A) $\theta_i = 78.000^\circ$, (B) $\theta_i = 78.463^\circ$.

78.925° with level 31.45 dB and the 1st order diffraction becomes the second largest one at 127.439° with 30.52 dB. Slightly changing θ_i from 78.000° to 78.463° , we have Fig. (B), where the -1st order diffraction appears at 78.463° with 31.89 dB in level, which is slightly (0.44 dB) higher than the -1st order diffraction peak in Fig. (A). The 1st order diffraction peak appears at 126.870° with level 24.03 dB, which is 6.49 dB down in level from that of Fig. (A). The largest -1st order diffraction peak is almost same in level in these figures, but the 1st order diffraction peak becomes lower in case of the critical $\theta_i = 78.463^\circ$. Thus, we may conclude that, the dip of p_c is caused by a fact that the 1st order diffraction peak is reduced at a critical angle $\theta_i = 78.463^\circ$.

7. Conclusions

We studied the scattering of a TM plane wave from a periodic surface with finite extent. To analyze efficiently a case with the corrugation width much larger than wave length, we proposed an undersampling approximation method. Then, we demonstrated that our method works practically for a slightly rough sinusoidal surface. In fact, we calculated the scattering cross section for a corrugation width up to $W/\lambda = 6.4 \times 10^3$. From numerical results, we newly found multiple scattering effects appear as strong dependence of the total scattering cross section per unit surface on the cor-

rugation width for a critical angle of incidence.

We also express our expectation such that the total scattering cross section per unit surface converges to the total diffraction cross section per unit surface, when the corrugation width tends to infinity. Our numerical results show that this expectation holds with high accuracy when the angle of incidence is non-critical but approximately for a critical angle of incidence. However, they suggest that the convergence is fast in case of a non-critical angle but is very slow in a critical case. To make this point clear, further numerical calculations are needed for much wider corrugation width.

We dealt with a special case, that is a sinusoidal corrugation with slightly rough and gentle slope. It is interesting to apply the undersampling approximation to a non-sinusoidal case. However, the applicability of the undersampling approximation is not clear at present[†]. However, we are interested in developing an analytical theory on the basis of the undersampling approximation. We are also interested in application of the undersampling approximation to a two-dimensional scattering problem [23], where the reduction of matrix size is essentially important for practical numerical calculations. However, these problems are left for future study.

References

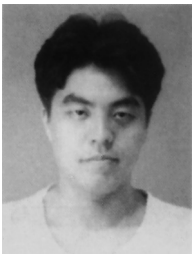
- [1] J. Nakayama and H. Tsuji, "Wave scattering and diffraction from a finite periodic surface: Diffraction order and diffraction beam," *IEICE Trans. Electron.*, vol.E85-C, no.10, pp.1808–1813, Oct. 2002.
- [2] J. Nakayama and Y. Kitada, "Wave scattering from a finite periodic surface: Spectral formalism for TE wave," *IEICE Trans. Electron.*, vol.E86-C, no.6, pp.1008–1105, June 2003.
- [3] M. Born and K. Huang, *Dynamical theory of crystal lattices*, Oxford Univ. Press, London, 1954.
- [4] J. Nakayama, "Wave scattering from an apodised sinusoidal surface," *IEICE Trans. Electron.*, vol.E83-C, no.7, pp.1153–1159, July 2000.
- [5] K. Hattori and J. Nakayama, "Scattering of TE plane wave from periodic grating with single defect," *IEICE Trans. Electron.*, vol.E90-C, no.2, pp.312–319, Feb. 2007.
- [6] M.E. Knotts and K.A. O'donnell, "Anomalous light scattering from a perturbed grating," *Opt. Lett.*, vol.15, no.24, pp.1485–1487, Dec. 1990.
- [7] J. Nakayama and L. Gao, "Diffraction and scattering of a plane wave from a randomly deformed periodic surface," *IEICE Trans. Electron.*, vol.E80-C, no.11, pp.1374–1380, Nov. 1997.
- [8] K. Hattori, J. Nakayama, and H. Matsuoka, "Wave scattering from a periodic random surface generated by a stationary binary sequence," *Wave in Random Media*, vol.11, no.1, pp.1–20, 2001.
- [9] R. Petit, ed., *Electromagnetic theory of gratings*, Springer, Berlin, 1980.
- [10] H. Ikuno and K. Yasuura, "Improved point-matching method with application to scattering from a periodic surface," *IEEE Trans. Antennas Propag.*, vol.AP-21, no.5, pp.657–662, 1973.
- [11] J. Yamakita and K. Rokushima, "Scattering of plane waves from dielectric gratings with deep grooves," *IECE Trans. Commun. (Japanese Edition)*, vol.J66-B, no.3, pp.375–382, March 1983.
- [12] J. Nakayama, Y. Ochi, and Y. Tamura, "Scattering of a TM plane wave from a periodic surface with finite extent: Perturbation solution," *IEICE Trans. Electron.*, vol.E89-C, no.9, pp.1358–1361, Sept. 2006.
- [13] K.W. Strutt, (Lord Rayleigh), *The theory of sound*, vol.2, Dover, New York, 1945.
- [14] S.O. Rice, "Reflection of electromagnetic waves from slightly rough surface," *Commun. Pure Appl. Math.*, vol.4, pp.351–379, 1951.
- [15] D. Maystre, "Rigorous theory of light scattering from rough surfaces," *J. Optics (Paris)*, vol.15, no.1, pp.43–51, 1984.
- [16] A. Kashiara and J. Nakayama, "Scattering of TM plane wave from a finite periodic surface," *IEICE Trans. Electron. (Japanese Edition)*, vol.J88-C, no.7, pp.493–501, July 2005.
- [17] M. Tomita, T. Sakashita, and Y. Karasawa, "Analysis of scattering problem by an imperfection of finite extent in a plane surface," *IEICE Trans. Electron.*, vol.E88-C, no.12, pp.2177–2191, Dec. 2005.
- [18] J. Nakayama and A. Kashiara, "Energy balance formulas in grating theory," *IEICE Trans. Electron.*, vol.E86-C, no.6, pp.1106–1108, June 2003.
- [19] M.I. Charnotskii, "Wave scattering by periodic surface at low grazing angles: Single grazing mode," *Progress in Electromagnetic Research, PIER 26*, pp.1–42, 2000.
- [20] J. Nakayama, K. Hattori, and Y. Tamura, "Diffraction amplitudes from periodic Neumann surface: Low grazing limit of incidence," *IEICE Trans. Electron.*, vol.E89-C, no.5, pp.642–644, May 2006.
- [21] J. Nakayama, K. Hattori, and Y. Tamura, "Diffraction amplitudes from periodic Neumann surface: Low grazing limit of incidence (II)," *IEICE Trans. Electron.*, vol.E89-C, no.9, pp.1362–1364, Sept. 2006.
- [22] J.A. DeSanto, "Scattering from a perfectly reflecting arbitrary periodic surface: An exact theory," *Radio Science*, vol.16, no.6, pp.1315–1326, 1981.
- [23] J. Nakayama, "Periodic Fourier transform and its application to wave scattering from a finite periodic surface: Two-dimensional case," *IEICE Trans. Electron.*, vol.E88-C, no.5, pp.1025–1032, May 2005.

[†]To estimate the applicability of the undersampling approximation, we have carried out numerical calculations for several values of the roughness parameter σ . In the case where $N_Q = 6$, $L = 2.5\lambda$ and $W = 6400\lambda$, we found that E_{rr} increases as σ increases. But E_{rr} is less than 1% for any angle of incidence if $\sigma \leq 0.4\lambda$. When $\sigma = 0.4\lambda$, the slope parameter becomes $2\pi\sigma/L = 2\pi \times 0.4/2.5 \approx 1$, which is approximately twice as much as the Rayleigh limit $2\pi\sigma/L = 0.448$. This fact agrees with Petit's result [9] for the perfect sinusoidal case, who found that numerical analysis based on the Rayleigh hypothesis is reliable even if the slope parameter is twice as much as the Rayleigh limit. It should be noticed that these discussions are essentially restricted to the far field, because they are carried out on the basis of the optical theorem or the energy conservation. Furthermore, there is no other source to compare with our results at present. Thus, further works are required to determine the applicability of the undersampling approximation.



Junichi Nakayama received the B.E. degree from Kyoto Institute of Technology in 1968, M.E. and Dr. Eng. degrees from Kyoto University in 1971 and 1982, respectively. From 1971 to 1975 he worked in the Radio Communication Division of Research Laboratories, Oki Electric Industry, Tokyo. In 1975, he joined the staff of Faculty of Engineering and Design, Kyoto Institute of Technology, where he is currently Professor of Electronics. From 1983 to 1984 he was a Visiting Research Associate in Department of

Electrical Engineering, University of Toronto, Canada. Since 2002, he has been an Editorial Board member of *Waves in Random and Complex Media*. His research interests are electromagnetic wave theory, acoustical imaging and signal processing. Dr. Nakayama is a member of IEEE and a fellow of the Institute of Physics.



Yasuhiko Tamura received the B.E., M.E., Ph.D. degrees from Kyoto Institute of Technology in 1991, 1993 and 2005, respectively. From 1993 to 1994, we worked in Technical Research Center, Konami, Co. Ltd., Kobe. In 1994, he joined the staff of Faculty of Design and Engineering, Kyoto Institute of Technology. His research interests are electromagnetic wave theory, computational method for stochastic analysis and visualization of electromagnetic field. Dr. Tamura received the Paper Presentation Award from Institute of Electrical Engineering of Japan in 1996.